

UDC 66.047.63:621.57

## MODELING OF GRAIN DRYING PROCESS BY ROTATING THERMOSYPHON

A. V. Zykov, I. V. Bezbakh, P. I. Osadchuk  
Odessa National Academy of Food Technologies

*The mathematical model for periodic drying of wheat in a contact dryer with rotating thermosyphon allows designing the drying process in unsteady conditions. Besides, the model expands the drying process concept by using the auxiliary process deceleration mechanism. It is associated with the reduction in water bridges' radii of curvature formed on the surfaces contacts. Simulation results and comparison with the experimental data are presented and argued.*

**Key words:** grain drying; heat and mass transfer; mathematical modeling.

**Introduction.** The system with a rotating thermosyphon (RTS) was developed by Burdo [1] (Burdo et al., 2008) and coauthors [2] (Gajda et al., 2000) for the thermal treatment of bulk materials. A dryer with RTS (Fig. 1) comprises housing (1), a condenser (2), a vapor generator (3) a driver (4). RTS is a hermetically sealed cavity partially filled with working fluid executing a closed evaporation-condensation cycle. RTS performs energy transfer from an external source to the grain layer. RTS also produces intense mixing of layer that promotes regeneration of the interface and obliteration of the heat and diffusion boundary layers. It was necessary the authors for comparison with experimental data with whole experimentation details to use. The short drying theory state analysis is presented lower.

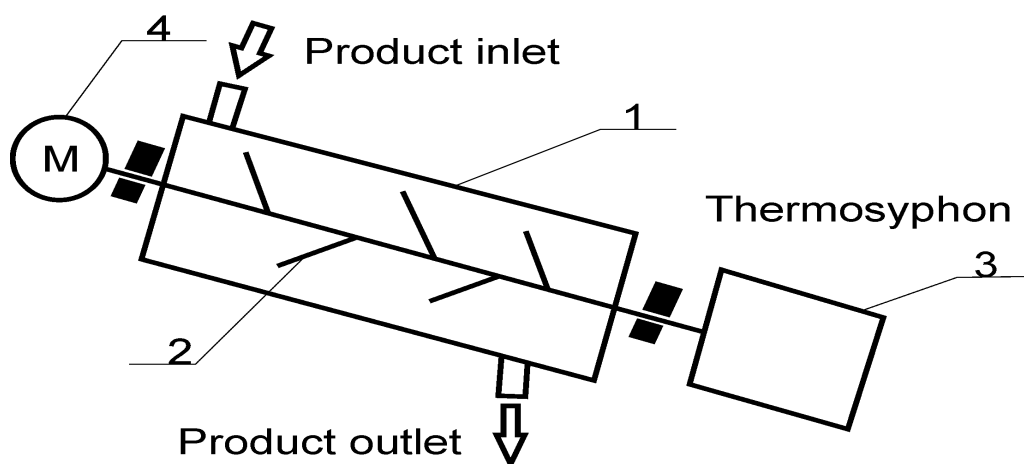


**Fig 1.** RTS system layout. 1 - housing, 2 - condenser, 3 - vapor generator, 4 – driver.

**Analysis of recent researches and publications.** Currently, different approaches are in use for drying process simulation. Fundamentals of Drying were introduced by Lykov [3–5] (1965, 1966, 1975) and Whitaker [6] (1977). Xiao Dong Chen and Arun S. Mujumdar [7] (2008) reviewed modern developments and applications of the models of Drying. Antonijevic (2009) [8] presented a one-dimensional model

based on the Lykov approach, neglecting the pressure gradient affects to heat and mass transfer. The model does not count for the internal heterogeneity of grain layer. It appears promising to account the internal mass transfer by augmenting the Whitaker model with the bound moisture concept introduced by Erriguible et al (2005) [9]. However, in the first drying period, the accounting of the external heat and mass transfer is more important. It is possible to solve this problem by determining the boundary layer thickness from the Navier-Stokes equations. Thus, Curcio Stefano (2010) [10] applied CFD methods for modeling of the solid materials drying. Jamaledine and Ray (2010) [11] consider possibilities of applying CFD for simulations of dispersed materials drying. It is possible to study an interaction between the grain layer and the air as the double-flow model (Euler-Euler) or an interaction between the flow and individual particles (Euler - Lagrange). The choice of the model depends on the properties of the drying object. Grain is a capillary-porous colloidal body that is why diffusion, semi-empirical and empirical drying models are used mainly. Barrozo et al. (2006) [12] showed that basing on the grain surface structure, modelling of heat and mass transfer with the drying agent (boundary conditions) embodies the correlations between the dimensionless numbers Nu, Sh and Re, Pr, Sc. Also, Hemis et al. (2009) [13] suggested using the Lewis equation. Bathiebo et al. (2009) [14] analyzed the conductive heat input to the side surface of the cylindrical chamber. Simulations of the unsteady temperature field at the conductive energy input are given by Jian-Hua Yan et al. (2009) [15]. Tsotsas et al. (2007) [16] introduced the model of sharp drying front distribution from the walls to the deeper layers. The key problem of this model is unknown time of the ideal mixing.

**Problem.** So unfortunately, the authors did not discover among many publications any propositions contained the new deepened prescription of the moving particles layer drying physical mechanisms including it discussion and comments with their drawbacks and advantages.

**The purpose of the research.** The approach main essence is the paper key aim. The author approach main positions are the next:

The whole thermal regimes mathematical prescription & modeling, including the temperature unsteady field moments. The moisture air dynamic state development prescription. The water content inside the grain volume changing modeling, with respect of common heat & mass transfer prescription and humid air flow filtration from the drying object internal volume into environmental media. The moisture content on the external surfaces of the drying object volume dynamic modeling and the process influence on common moisture content changing. The drying object water content changing under it mixing with RTS rotation respect modeling prescription. The author approach was limited the moisture drying only from the external surfaces inside object; though in many cases it is only small water content part. It is connected mainly with absence of total necessary information about the moisture state at these object parts.

**Assumptions and structure of the model.**

The following assumptions are needed for the model statement:

- heating of the layer is accomplished through the contact between the rotating heating surface and the heated material;
- the drying material is non-deformable;
- evaporation occurs within the heated zone only;
- due to variations of the layer parameters in the radial direction only, the one-dimensional model could be considered.

First, unsteady temperature fields in the object should be calculated with respect to the energy source type and its thermal connections to the drying object. At this stage, the equilibrium conditions are also recorded at the interfaces, i.e. on evaporation surfaces. At the following stage, basing on the media structure data the modes of vapor and air flows in the grain layer are defined by means of the Fick's and Darcy's Laws. Then, the basic correlations between temperature distributions and parameters determined by the "driving forces" of local mass transfer processes should be analyzed. As the next step, the authors suggest introducing the auxiliary equations accounting for the deteriorating of "driving forces" throughout the drying process. This is associated with elements of the moisture remaining in the contact areas of the grains. During drying the moisture layer both thickness in these zones and curvature radii of surfaces at these locations are reduced. As a result, this leads to an increase in capillary pressure and, consequently, reduces both vapor pressures over the material surface and the driving forces. At the final stage, the calculation equations should be combined into the general model, and decrease of moisture should be determined.

#### **Models of layer temperature distributions at the unsteady heating.**

To determine the average temperature of the heated grain layers under unsteady heating of the system, the equation of energy conservation should be used. The equation comprises the RTS mass  $M_1$  and the heat capacity  $C_1$ ; mass  $M_2$  and the heat capacity  $C_2$  of the working fluid inside the RTS; mass  $M_3$  and heat capacity  $C_3$  of the grain layer. Taking into account the heat losses to the surroundings, the equation appears as follows:

$$Q = [M_1 \cdot C_1 + M_2 \cdot C_2 + M_3 \cdot C_3] \cdot \frac{dt_1}{d\tau} + \alpha_3 \cdot S_{32} \cdot [t_1 - t_s] \quad (1)$$

Here  $S_{32} = (1 - k_3) \cdot S_3$  - part of the RTS outer surface removing heat to the surroundings,  $t_1$  and  $t_{oc}$  - temperatures of the RTS surface and surroundings, respectively.  $\alpha_3$  - the heat transfer coefficient from the container surface to the environmental media,  $k_3$  any coefficient, what is accounted the external surface RTS part, what have direct contact with environmental media.

Its solution has the following form:

$$t_1 - t_s = \frac{A_1}{B_1} \cdot [1 - \exp(-B_1 \cdot \tau)]$$

$$A_1 = Q / [M_1 \cdot C_1 + M_2 \cdot C_2 + M_3 \cdot C_3] \quad (2)$$

$$B_1 = \alpha_3 \cdot S_{32} / [M_1 \cdot C_1 + M_2 \cdot C_2 + M_3 \cdot C_3]$$

$A_1$  and  $B_1$  are constants depending on the properties of a heater and grain layer and heat exchange conditions. The initial drying period for the present technology is

associated with the unsteady heating mode. The important point is the analysis of the temperature distribution in the heated grain layer. This corresponds to the following layer thickness:

$$\delta_0 = \sqrt{C_0 \cdot a_e \cdot \tau_i} \quad (3)$$

It was suggested, that the effect of stirring layer should be accounted by the analogy with the influence of turbulent mixing on the rate of heat transfer in the turbulent fluid jets (Isachenko, 1977 [17]), (Carslaw and Jaeger, 1959 [18]):

$$a_e = a_0 + \varepsilon_0 \cdot W_i \cdot L \quad (4)$$

The equation (4) was suggested by the authors to use, as it was proposed the analogy existence between transfer momentum and heat values.

$C_0$  – in (3) is empirical coefficient equal approximately 2.

It is assumed that characteristic size is equal to the overall thickness of the layer:  $L = \delta_{30}$ . The system of heat conduction correlations for this problem is as follows:

$$t_{1i} = t_s + Z_{11i} \cdot (t_{1i} - t_s) \quad (5)$$

$$Z_{11i} = \operatorname{erf} \left( \frac{1}{2\sqrt{Fo_i}} \right) - \exp \left[ \frac{\alpha_{22}}{\lambda_{\phi}} \cdot L_1 \cdot \frac{(a_{22})^2}{(\lambda_{\phi})^2} \cdot a_e \cdot \tau_i \right] \cdot \operatorname{erfc} \left[ \frac{1}{2\sqrt{Fo_i}} + \frac{\alpha_{22}}{\lambda_{\phi}} \sqrt{a_e \cdot \tau_i} \right] \quad (6)$$

Knowing the temperatures in locations where evaporation is possible gives a basis for the calculation of the partial pressures and mass transfer "driving forces". The key equation is as follows:

$$P_{1i} = P_0 \cdot \exp(Z_{1i})$$

$$Z_{1i} = (r/R1) \cdot \left( \frac{1}{t_s} - \frac{1}{t_{1i}} \right) \quad (7)$$

### Models of vapor-air mixture movement from the inner volume of the material layer.

It is assumed that the increased pressure occurs in the layer as a result of moisture evaporation from the surface of the grain. This leads to the filtration of vapor-air mixture through the material layer to the surroundings. It is described by the linear Darcy law:

$$W_{1i} = \frac{\Delta P_{1i} \cdot K_{fi}}{S_{1i} \cdot \mu_{1i}} \quad (8)$$

Determination of permeability at the known data on layer structure (grain size, layer porosity) is possible by means of the Carman-Kozeny or similar equations, having a form as:

$$K_{fi} = \operatorname{const} \cdot \varepsilon_i^3 \cdot D_0^2 / (1 - \varepsilon_i)^2 \quad (9)$$

Gorbis (1970) [19] proposed to analyze mass transfer processes at evaporation inside the layer by means of the following correlation:

$$Nu_D^1 = 2.35 \cdot Pe_D^{0.38} \cdot (L/D_t)^{0.4} \quad (10)$$

Mass flow density in the "moving heated zone" is defined by the equation of mass transfer:

$$j_{E1} = \beta_p \cdot (\alpha_w P_w - P_{Ei}) \cdot S_y \cdot (2 \cdot \delta_{bi} \cdot \pi \cdot D_t + \delta_{bi}^2) \cdot L_t \quad (11)$$

There are at an equation (11):  $\beta_p \cdot (\alpha_w P_w - P_{Ei})$  - the specific mass transfer from the unit volume of the drying object surface;  $S_y \cdot (2 \cdot \delta_{bi} \cdot \pi \cdot D_t + \delta_{bi}^2)$  - value of specific the mass transfer surface on the length RTS unit;  $L_t$  - the RTS working length. Thus, the drying process calculation algorithm has been created. Procedures accounting for the emergence of mechanisms suppressing intensity of the process and causing deceleration represent essential supplementary elements of this algorithm.

### **The model of "capillary deceleration mechanism" formation for grain layer drying.**

It is assumed that capillary deceleration mechanism is associated with the removal of moisture from the surface. In the case that has been studied by the authors, the evaporation of moisture from the surface of the grains leads to a reduction of its volume and, as a consequence, to the thinning of some liquid film. Subsequently, the liquid film moves to the layer bottlenecks, i.e. to the contact areas between individual grains. Curved vapor-liquid interfaces "deepening" with evaporation rate growing occur at these contact areas. Increasing of the interfaces curvature leads to substantial values of "capillary pressure". This reduces the "driving force" of mass transfer process. Outline of the corresponding calculations has the following form:

$$V_i = M_i / \rho_0 = [(M_0 - M_{2i}) - \sum (\Delta M_i)] / (N_{li} \cdot m \cdot \rho_0) \quad (12)$$

Based on the certain surplus of the surface moisture, and assuming its distribution over the contact points of elements (grain) layer, the radius of curvature of a curved interface could be estimated assuming that the radius is related to the scale of the liquid volumes by the cubic law, i.e. :

$$R_{0i}^3 \approx const \cdot V_i \quad (13)$$

The defined value of the radius allows evaluating the resultant "capillary pressure":

$$\Delta P_{\sigma i} = 2 \cdot \frac{\sigma}{R_{0i}} \quad (14)$$

When the radius of curvature approaches radii of drained medium internal channels, moisture evaporation from the inner channels starts. This process is not considered in this paper.

### **Generalizing equations**

The calculation algorithm is based on the determination of the evaporation layer thickness by means of correlations (11) – (14) for each time interval, and solving a material balance set of equations accounting for the material flows in the heated layer (surface evaporation, filtration through the material layer, diffusion of vapor and air). The set of equations implementing the above mentioned algorithm is presented in the form (15) with subsequent deriving correlations (16) – (18).

$$\left\{ \begin{array}{l} \frac{dG1}{d\tau} = \beta [P_n - (P_{pv} + dP_{pv})] \cdot V \cdot S_y \\ \frac{dG2}{d\tau} = \frac{K_f}{\delta_{30} \cdot \mu} \cdot [(P_{sl} + dP_{sl}) - P_0] \cdot \rho_a \cdot S_y \cdot V \\ \frac{dG3}{d\tau} = \frac{D_{op}}{R_v T1} \cdot \frac{(P_{pv} + dP_{pv}) - P_{pv0}}{D_t - \frac{\delta_e}{2}} \cdot \pi \cdot L_t \cdot (D_t + 2\delta_e) \\ \frac{dG4}{d\tau} = \frac{D_{op}}{R_a T1} \cdot \frac{(P_{pv} + dP_{pv}) - P_{pv0}}{D_t - \frac{\delta_e}{2}} \cdot \pi \cdot L_t \cdot (D_t + 2\delta_e) \end{array} \right. \left\{ \begin{array}{l} dM = dG1 - dG2 - dG3 + dG4 \\ dM = dM_a + dM_v \\ dM_a = -\frac{1}{1+x} dG2 + dG3 \\ dM_v = dG1 - \frac{x}{1+x} dG2 - dG3 \end{array} \right. \quad (15)$$

The equations (15) system contains all main parts of the total water mass flow from the internal mass transfer surface during the drying, including direct evaporation from the wetted surface; the water mass flow filtration over whole drying object volume; the diffusion mass flows and main mass flows balances equations. It was added on the equations (16). Accounting that

$$P_{sl} = P_{pv} + P_{pa} \quad dP_v = \frac{R_v \cdot T1}{V_a} \cdot dM_v \quad dP_a = \frac{R_a \cdot T1}{V_a} \cdot dM_a \quad dP_{sl} = dP_a + dP_v \quad (16)$$

set of equations (15) is rearranged as

$$ZX28 \cdot dM_a^4 + ZX33 \cdot dM_a^3 + ZX34 \cdot dM_a^2 + ZX35 \cdot dM_a + ZX36 = 0 \quad (17)$$

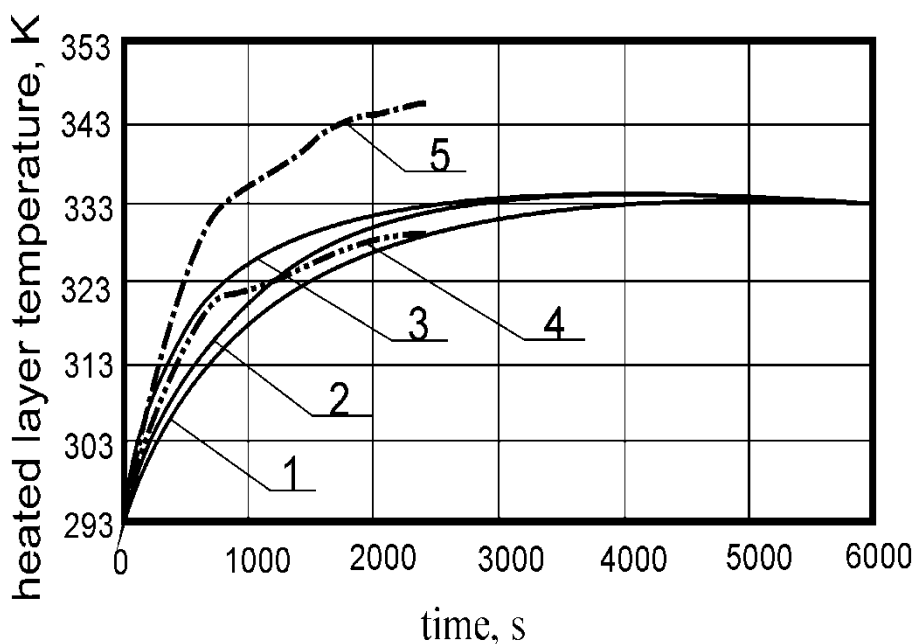
The solution represents changing of layer dry air mass during time interval  $\Delta\tau$ . It yields the removed moisture amount as

$$dG1 = \left[ dG3 + dM_v - \frac{dM_a \cdot (M_v + dM_v)}{M_a + dM_a} \right] \quad (18)$$

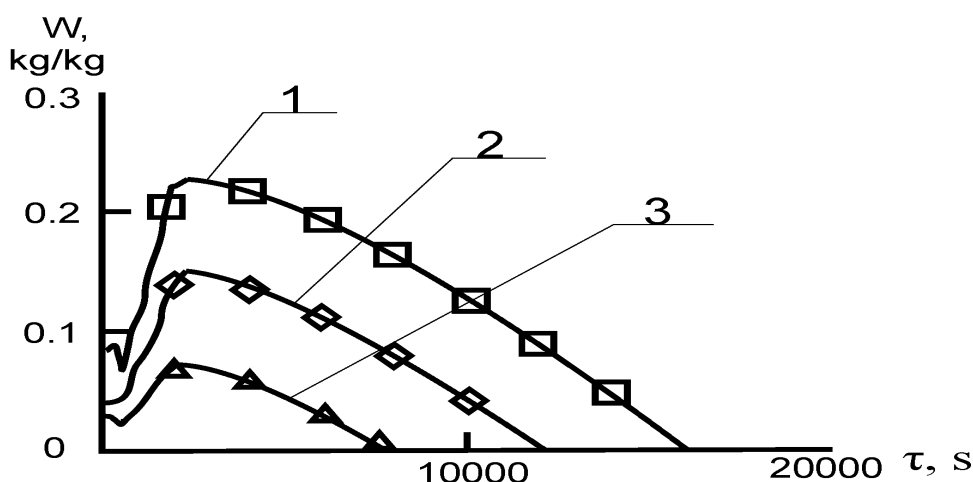
Since changing of the layer mass is caused by moisture removal ( $\Delta M = dG1$ ) only, then using of correlations (12) - (14) allows determining the driving force reduction at surface moisture evaporation due to capillary deceleration. The defined value of the driving force reduction should be accounted by the subsequent time interval calculation.

### Results and Discussion.

For objective justification of the proposed approach, experimental data on the grain layer drying obtained by Bezbach and Burdo (1999) [20] and Voskresenskaya (2010) [21] have been used. Drying of wheat and amaranth was performed in the experiments at mass load 10 kg and heat input ranged from 150 to 190 watts. The RTS dimensions were as follows: diameter of the core RTS channel - 20 mm; number of RTS peripheral branches - 20; RTS peripheral branches external diameter - 12 mm; number of revolutions varied from 30 to 40 rpm; overall drying time - 4000 – 6000 s; working fluid mass 0.5 kg; RTS weight - 2 kg. Comparison of simulation results with experimental data shows a significant dependence of the heating dynamics from the layer porosity (Fig. 2). There were presented in the figures simulations results for the case, when moisture on the grain external surface mainly located with 50% from total moisture only. It was the authors approach first step. The next one was connected with the study on the same base how simulation results changed by the significant the mentioned external moisture value changing. These results are presented mainly in Fig. 8, 9 and discussed in addition.

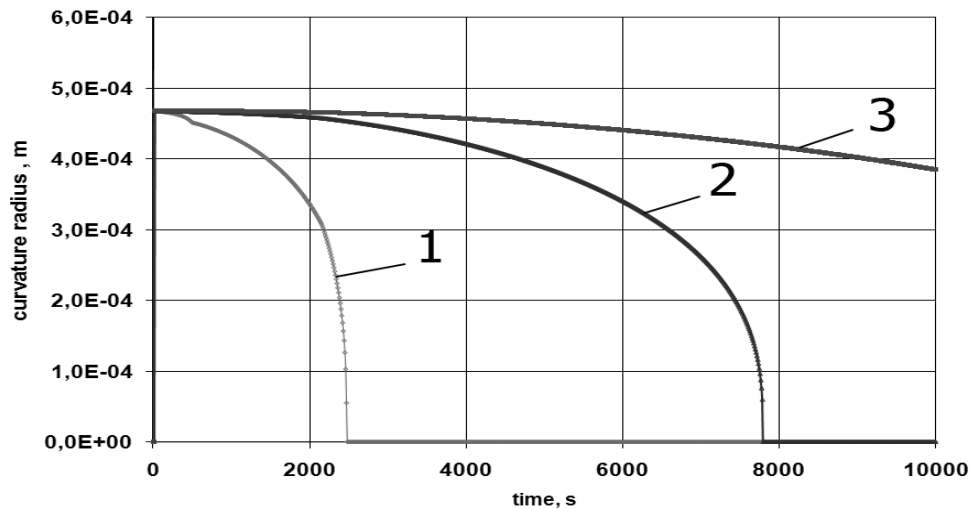


**Fig.2.** Dynamics of grain layer heating. 1- simulation results with layer porosity is assumed equal to 0.7; 2 - simulation results with layer porosity is assumed equal to 0.9; 3 - simulation results with layer porosity is assumed equal to 0.99; 4, 5 – experimental data.

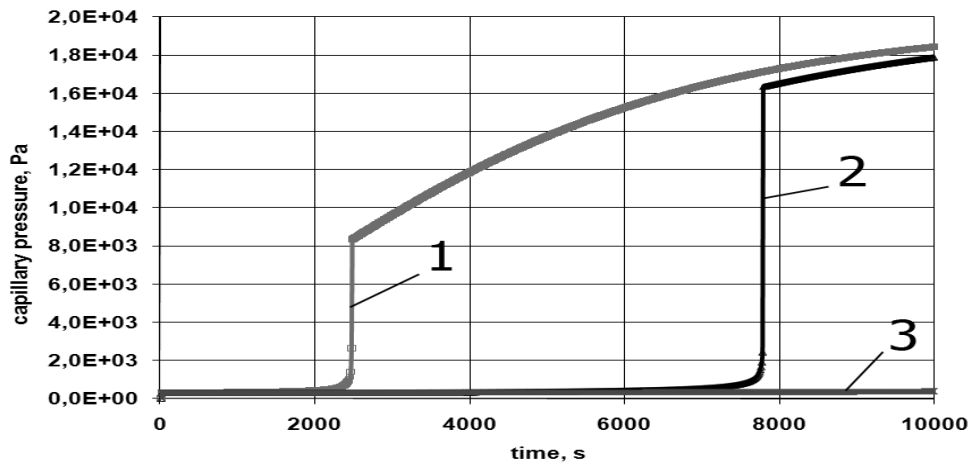


**Fig. 3.** Time dependence of outer grain surface moisture mass. 1- simulation results with layer porosity is assumed equal to 0.7; 2 - simulation results with layer porosity is assumed equal to 0.8; 3 - simulation results with layer porosity is assumed equal to 0.9.

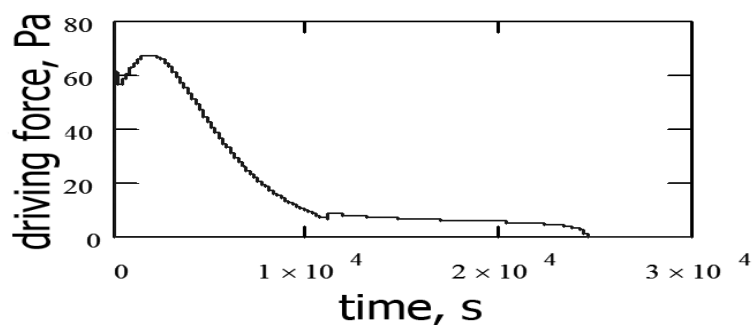
Figure 3 shows typical calculating results for time dependence of moisture amount change on the outer surface of the grain layer. Increase of the moisture mass in the "moving heated layer" is evident within about 300 seconds. This is due to the heated layer volume escalation. Then, when the point where the thickness of the "heated layer" becomes equal to the thickness of the entire layer is attained, sharp change in the trend is observable. It should be noted that the calculation data shown in Fig.3 are obtained when the outer surface moisture is equal to 50% of the entire moisture; the layer porosity is assumed equal to 0.7 (Wv07); 0,8 (Wv08) and 0,9 (Wv09).



**Fig. 4.** Time dependence of the radius of curvature. 1- simulation results with layer porosity is assumed equal to 0.99; 2 - simulation results with layer porosity is assumed equal to 0.9; 3 - simulation results with layer porosity is assumed equal to 0.7

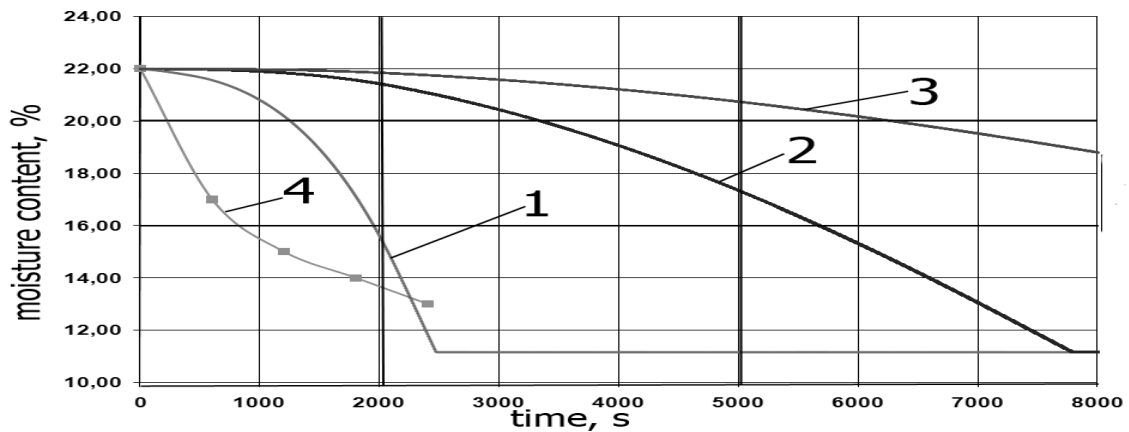


**Fig. 5.** Time dependence of the capillary pressure. 1- simulation results with layer porosity is assumed equal to 0.99; 2 - simulation results with layer porosity is assumed equal to 0.9; 3 - simulation results with layer porosity is assumed equal to 0.7.



**Fig. 6.** Time dependence of the driving force.

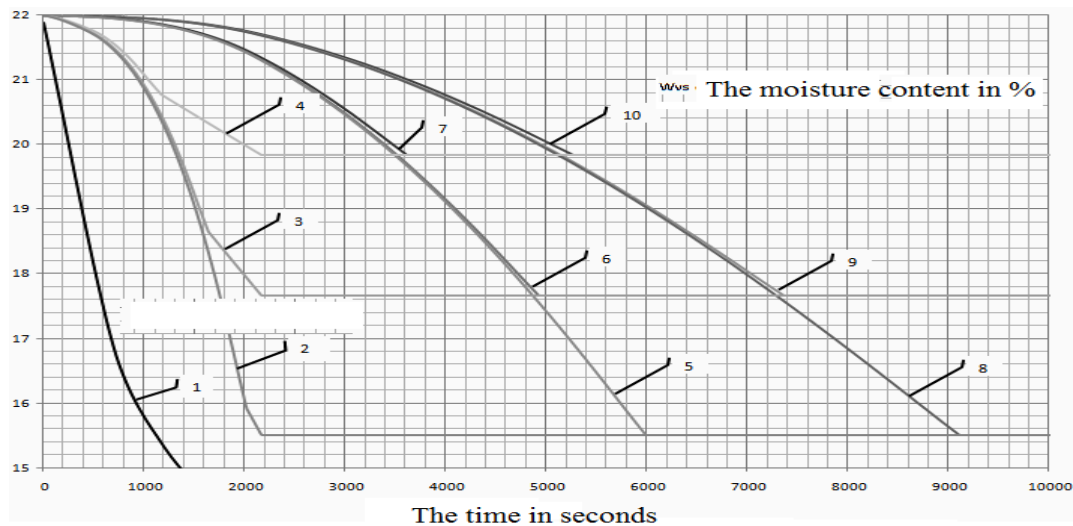




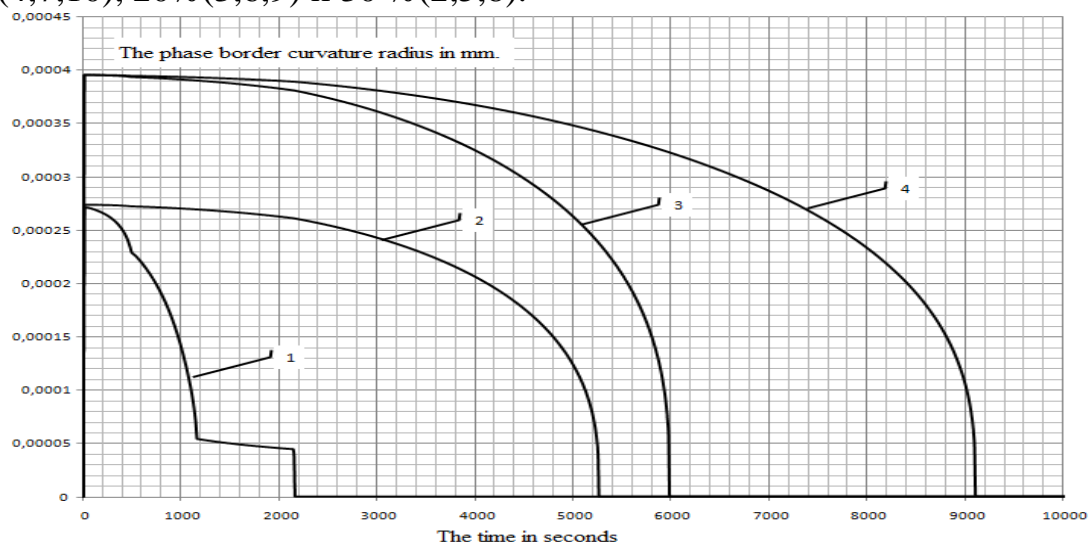
**Fig. 7.** Time dependence of moisture content. 1- simulation results with layer porosity is assumed equal to 0.99; 2 - simulation results with layer porosity is assumed equal to 0.9; 3 - simulation results with layer porosity is assumed equal to 0.7; 4 – experimental data.

Figure 4 shows time dependences of the “deepened meniscus” radii of curvature calculated at different values of stirred grain layer porosity (0.7, 0.9, and 0.99). Figure 5 presents data on the dynamics of capillary pressure over deepened meniscus calculated at different values of stirred grain layer porosity (0.7, 0.9, and 0.99). It was assumed that moisture content on the outer surface of the grain layer is 50%. The calculation data on time dependence of the mass transfer driving force at the layer porosity equal to 0.5 are showed in Figure 6. Figure 7 demonstrates calculation data on the dynamics of stirred grain layer moisture content at various initial data: 1. Fixed stirred grain layer porosity (0.7, 0.9, and 0.99). 2. Fixed moisture content on the outer surface of the grain layer is 50%. As can be seen, the decrease of moisture content on the outer surface leads to reduction of the curvature radius at the interface, and it is accompanied by capillary pressure increase and a corresponding decrease of mass transfer driving force. This in turn leads to a sharp reduction in the rate of moisture removal. The simulations results presented in the figures 8, 9 shown:

1. The essential external moisture decreasing was leading to the best agreement between the calculations and experimental results.
2. There is positive influence on the agreement the porosity increasing.
3. The authors understood that the mentioned problems in the comparison between experimentation and simulation results are needed in the next step in their approach development. We considered, that the most important in it: It is connected with the necessity to account right many key moments in the grain layer drying at the experimental RTS rotating dryer, including the essential mixing of the grain volume, the layer porosity serious changing and etc.



**Fig. 8.** The dependency of any moisture on internal surface changing on porosity & initial it value influence during time. 1 – Experimentation data, 2,3,4 – the layer porosity value 99%; 5,6,7 - the layer porosity value 90%; 8,9,10 - the layer porosity value 80%; by the moisture initial content on the surface – 10% (4,7,10), 20% (3,6,9) и 30 % (2,5,8).



**Fig. 9.** The phase border curvature radius (in mm.) changing dependency on time (in seconds) for different porosities & initial moisture content. The porosity: 1- 99%, 3 – 90%, 2,4 – 80% and internal moisture initial content 1,2 – 10%, 3,4 – 30%.

**Conclusions.** In spite of afore mentioned problems and drawbacks in the comparison between simulation and experimentation the authors are considering the next. The proposed mechanism of deceleration is a new step in the description of the drying process. It is useful for a deeper analysis of the internal phenomena of drying. Taking into account the impact of the mechanism the authors want to pay attention to the following: 1. Forms of moisture inside the object depend on the method of penetration and distribution of moisture into the material, the ratio between the moisture amounts in the outer and inner surfaces of the channels. 2. A specific example of drying selected by the authors for comparison with the experimental data showed that the suggested physical mechanism of deceleration does demonstrate the effect. Its quantitative appearance depends on the ratio of the

moisture content on the external and internal surfaces. For a grain layer it is the sum of the surfaces of individual grains. Also it depends on the permeability and the internal structure of the grain layer. 3. There may be other physical mechanisms affecting the kinetics of the process. In order to at least qualitatively describe such mechanisms, we need comprehensive information on the forms of the moisture content in the internal volumes, size of the moisture removing channels, their distributions, etc. Such information requires complex experiments, but it is necessary to obtain objective data about other mechanisms of suppressing the intensity of the drying process. However, further in-depth study of drying mechanisms is impossible without this information. 4. The authors are planning, that at the nearest future they should be trying to apply their approach for the corresponding analysis of the other objects drying cases, using whole data from publications. 5. To develop more and in detail the approach with whole peculiarities processes heat & mass transfer inside RTS volume.

### REFERENCES

1. Burdo O.G., Bezbah I.V. Rotating heat pipes in devices for heat treatment of the food-stuffs. Applied Thermal Engineering, Volume 28, Issue 4, March 2008, Pages 341-343.
2. Gajda S., Zykov A. V., Burdo O. G. Application of heat pipes for bread baking and grain drying heat technologies perfecting. IV Minsk International Seminar "Heat Pipes, Heat Pumps, Refrigerators" Minsk, Belarus, September 4-7, 2000.
3. Luikov A.V. «Heat and Mass Transfer in Capillary – porous Bodies». p. 230, Pergamon Press, London, 1966.
4. Luikov A.V., Mikhailov I.A. "Theory of Energy and Mass Transfer", Pergamon Press, 392p., 1965.
5. Luikov, A.V. Systems of differential equations of heat and mass transfer in capillary-porous bodies. International Journal of Heat and Mass Transfer 1975, vol. 18, pp.1–14.
6. Whitaker, S. Simultaneous heat, mass, momentum transfer in porous media: A theory of drying. Advances in Heat Transfer, vol. 13, pp.119–203, 1977.
7. Xiao Dong Chen and Arun S. Mujumdar "Drying Technologies in Food Processing", Blackwell Publishing Ltd. pp.352, 2008.
8. Antonijevic, Dragi Variable Coefficients Model for Drying Processes with Conductive Heat Supply, Drying Technology, vol. 27: 1, pp. 71 — 75, 2009
9. Erriguible A., Bernada, P. , Couture F. and Roques M. -A. Modeling of Heat and Mass Transfer at the Boundary Between A Porous Medium and Its Surroundings, Drying Technology, vol. 23: 3, pp. 455 — 472, 2005.
10. Curcio Stefano A Multiphase Model to Analyze Transport Phenomena in Food Drying Processes, Drying Technology, vol. 28: 6, pp. 773 — 785, 2010
11. Jamaledine Tarek J. and Ray Madhumita B. Application of Computational Fluid Dynamics for Simulation of Drying Processes: A Review, Drying Technology, vol. 28: 2, pp.120 — 154, 2010.
12. Barrozo, M. A. S. , Murata, V. V. , Assis, A. J. and Freire, J. T. Modeling of Drying in Moving Bed, Drying Technology, vol. 24: 3, pp. 269 — 279, 2006

13. Hemis M. , Bettahar, A. , Singh, C. B. , Bruneau, D. and Jayas, D. S. An Experimental Study of Wheat Drying in Thin Layer and Mathematical Simulation of a Fixed-Bed Convective Dryer, *Drying Technology*, vol. 27: 10, pp. 1142 — 1151, 2009.
14. Bathiebo, J. , Daguinet, M. , Zeghmati, B. , Tolley, M. , Fodé, M. and Ouédraogo, A. Drying Corn Grains Contained in a Vertical Channel with Constant Heat Flux on Walls, *Drying Technology*, vol. 27: 3, pp. 459 — 466, 2009
15. Yan, Jian-Hua , Deng, Wen-Yi , Li, Xiao-Dong , Wang, Fei , Chi, Yong , Lu, Sheng-Yong and Cen, Ke-Fa Experimental and Theoretical Study of Agitated Contact Drying of Sewage Sludge under Partial Vacuum Conditions, *Drying Technology*, vol. 27: 6, pp. 787 — 796, 2009.
16. Tsotsas, E. , Kwapinska, M. and Saage, G. Modeling of Contact Dryers, *Drying Technology*, vol. 25: 7, pp. 1377 — 1391, 2007.
17. Isachenko V.P. «The condensation heat transfer», Publ. «Energy», M. 1977, 240 pp. (in Russian);
18. Carslaw H.S. & Jaeger J. C. *Conduction of heat in solids*, second edition, Oxford at the Clarendon Press, 1959, 486 pp.
19. Gorbis Z.R. “Dispersed flows Hydrodynamic & Heat Transfer” Publ. H. “Energy”, Moscow. 1970. 424 pp. (in Russian).
20. Bezbach I.V., Burdo O.G. “Thermomechanical Apparatus for Food Products treatment” / *Scientific Works OGAFT*. – 1999. Iss. 21. – pp. 234–237. (in Russian).
21. Voskresenskaya E.V. “The drying process dynamic peculiarity by Thermomechanical Apparatus using” // – Odessa, – *Scientific Works OGAFT*, – Iss. 37, – 2010, 81–84 (in Russian).

### **МОДЕЛИРОВАНИЕ ПРОЦЕССА СУШКИ ЗЕРНА В АППАРАТЕ С ВРАЩАЮЩИМСЯ ТЕРМОСИФОНОМ**

Зыков А.В., Безбах И.В., Осадчук П.И.

**Ключевые слова:** зерносушение, тепломассоперенос, математическое моделирование.

#### **Резюме**

*Математическая модель периодической сушки пшеницы в контактной сушилке с вращающимся термосифоном позволяет моделировать процесс сушки в нестационарных условиях. Кроме того, модель расширяет концепцию процесса сушки с помощью механизма замедления вспомогательного процесса. Это связано с уменьшением радиусов кривизны водных мостиков, образованных на контактах поверхностей. Представлены и аргументированы результаты моделирования и сравнение с экспериментальными данными.*

### **MODELING OF GRAIN DRYING PROCESS BY ROTATING THERMOSYPHON**

Zykov A. V., Bezbakh I. V., Osadchuk P. I.

**Key words** grain drying; heat and mass transfer; mathematical modeling.

### Summary

*The mathematical model for periodic drying of wheat in a contact dryer with rotating thermosyphon allows designing the drying process in unsteady conditions. Besides, the model expands the drying process concept by using the auxiliary process deceleration mechanism. It is associated with the reduction in water bridges' radii of curvature formed on the surfaces contacts. Simulation results and comparison with the experimental data are presented and argued.*